Presentation based on J. High Energ. Phys. (2018) 2018: 90

- Collaborated with **Qiang Li**
- With special thanks to **Kaoru Hagiwara**

Probing the Dark Sector through Mono-Z Boson Leptonic Decays

Daneng Yang

School of Physics, Peking University

Department of Physics, Tsinghua University

The 24th International Summer Institute on Phenomenology of Elementary Particle Physics and Cosmology

August 16th, 2018 Panshan, Tianjin

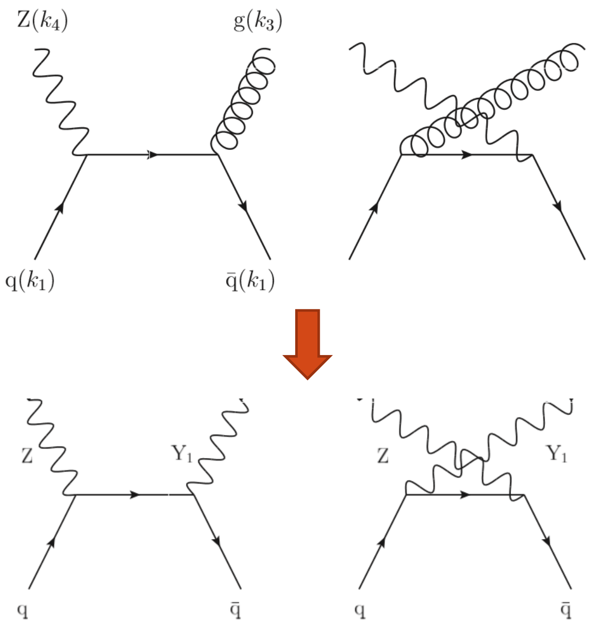

Motivation

Measuring angular coefficients of high pT Z boson leptonic decays

Z boson pT balanced by **jets** → Z boson pT balanced by **missing energy**

Angular coefficients of Z boson leptonic decays

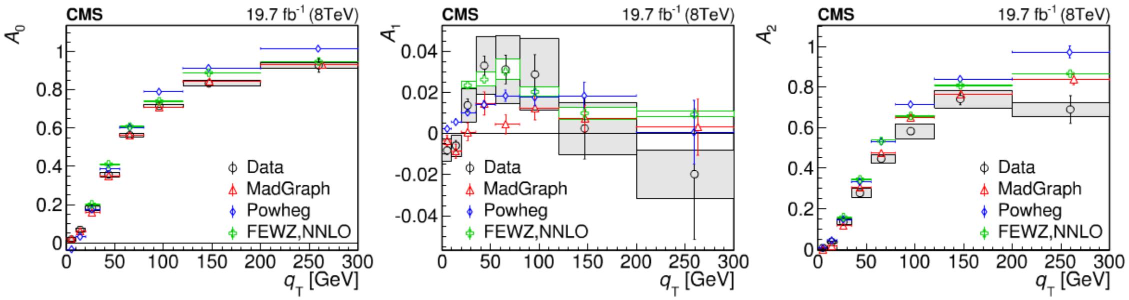

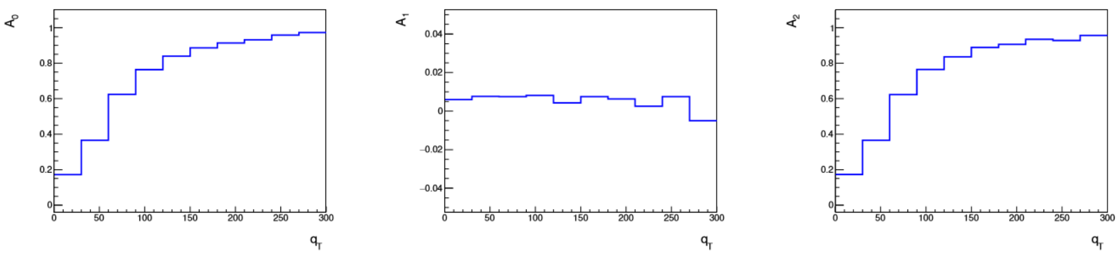

CMS: Phys. Lett. B 750 (2015) 154

ATLAS: JHEP08(2016)159

Order in QCD

0^{th} A4 only, from qqbar->Z

1^{st} A0-A4,

Lam–Tung relation: A0=A2

2^{nd} A0-A7, all appear

Comparison of the measured angular coefficients and the parton level predictions (L.O.)

- The Z boson e/mu decays have very clean signatures
- QCD corrections to angular coefficients are very small

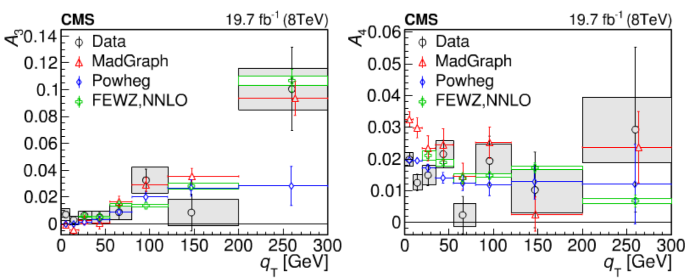

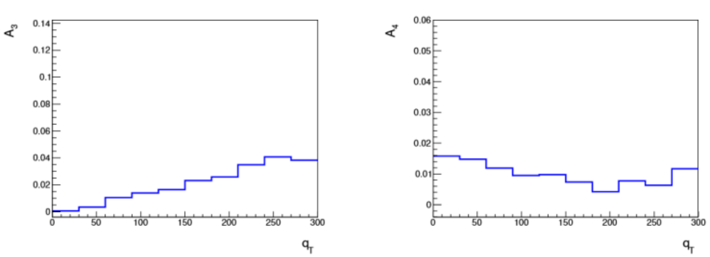

Angular coefficients in the Collins-Soper frame

$$\frac{d\sigma}{dq_T dy_Z ds_Z d\cos\theta d\phi} = \left(\int d\cos\theta d\phi \frac{d\sigma}{dq_T dy_Z ds_Z d\cos\theta d\phi}\right)\frac{3}{16\pi}$$

$$\left\{(1+\cos^2\theta) + \frac{1}{2}A_0(1-3\cos^2\theta) + A_1 \sin 2\theta \cos\phi + \frac{1}{2}A_2 \sin^2\theta \cos 2\phi + A_3 \sin\theta\cos\phi + A_4\cos\theta\right\}$$

- **Z + jet**
- **Z + dark matter**

Angular coefficients of Z boson leptonic decays

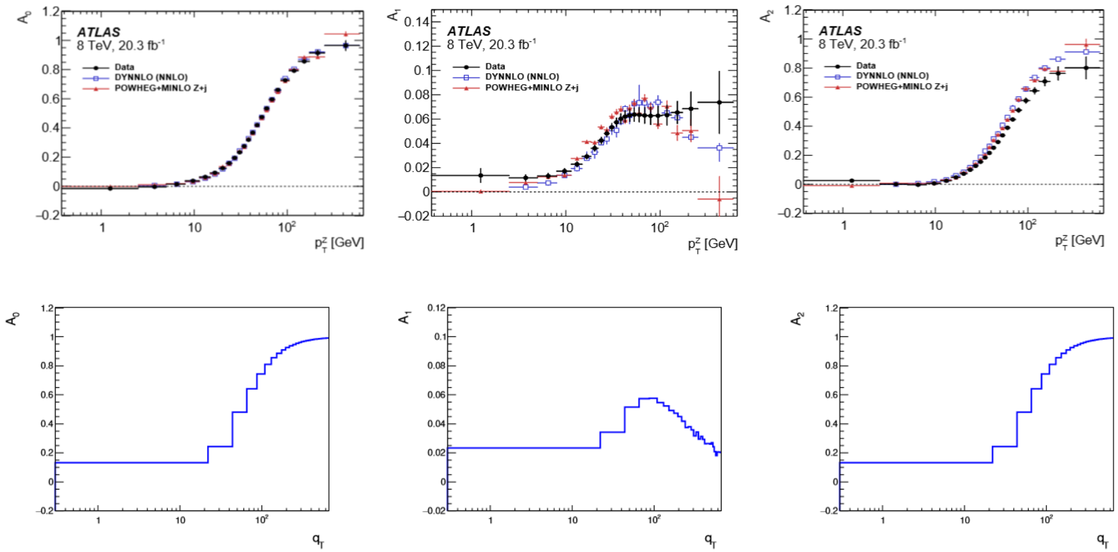

ATLAS: JHEP08(2016)159
CMS: Phys. Lett. B 750 (2015) 154

Order in QCD
0th A4 only, from qqbar->Z
1st A0-A4,
Lam–Tung relation: A0=A2
2nd A0-A7, all appear

Comparison of the measured angular coefficients and the parton level predictions (L.O.)

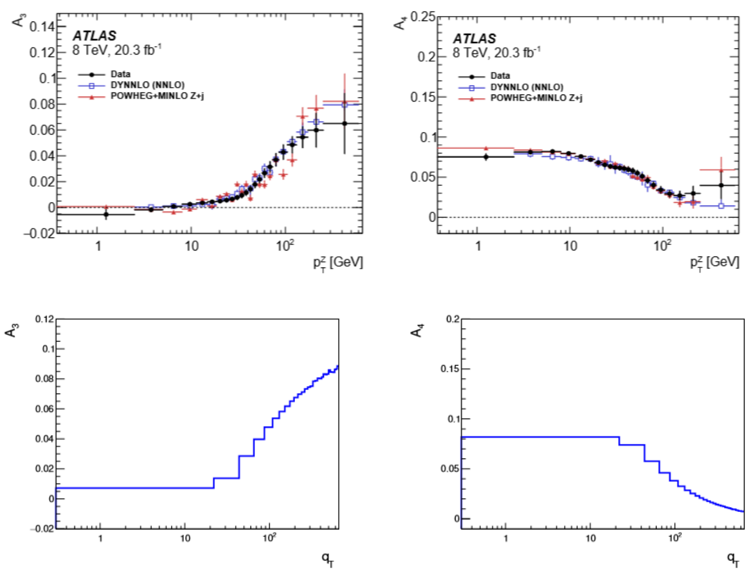

Angular coefficients in the Collins-Soper frame

- The Z boson e/mu decays have very clean signatures
- QCD corrections to angular coefficients are very small

$$\frac{d\sigma}{dq_T dy_Z ds_Z d\cos\theta d\phi} = \left(\int d\cos\theta d\phi \frac{d\sigma}{dq_T dy_Z ds_Z d\cos\theta d\phi}\right)\frac{3}{16\pi}$$
$$\left\{(1+\cos^2\theta) + \frac{1}{2}A_0(1-3\cos^2\theta) + A_1 \sin 2\theta \cos\phi + \frac{1}{2}A_2 \sin^2\theta \cos 2\phi + A_3 \sin\theta\cos\phi + A_4\cos\theta\right\}$$

- Z + jet
- Z + dark matter

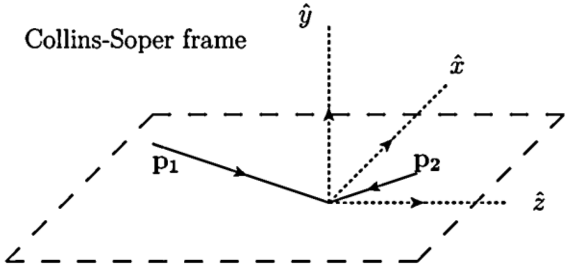

Parametrization of the lepton angular distribution

Measuring angular coefficients of high pT Z boson leptonic decays

Z boson pT balanced by **jets** → Z boson pT balanced by **missing energy**

Parametrization of the lepton angular distribution

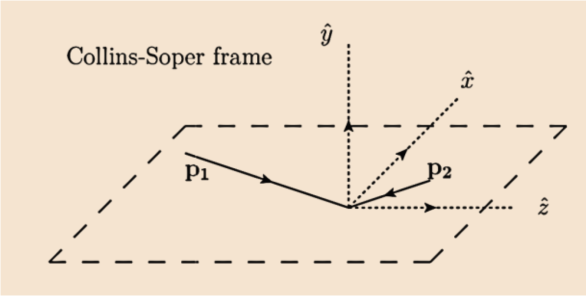

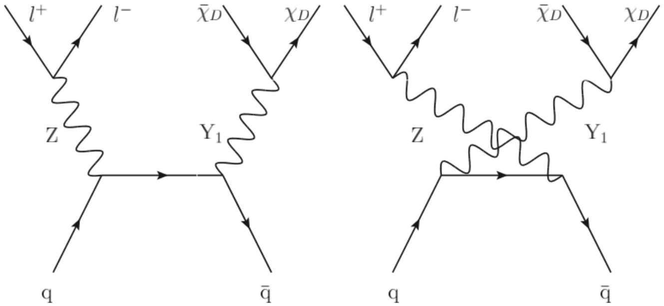

We parametrize the phase space as visible part

$$\mathbf{x} = (y_Z, q_T, \cos\theta_{CS}, \phi_{CS})$$

and invisible part

$$(y_Y, s_Y, \cos\theta_\chi, \phi_\chi)$$

x_1, x_2 fixed through delta functions

- The z-axis is defined as the bisector of the angle θ_{12} between $\mathbf{p_1}$ and $-\mathbf{p_2}$.
- $\tan\frac{\theta_{12}}{2} = \frac{q_T}{\sqrt{s_Z}}$, $q_T \equiv |\mathbf{q_T}|$:
  - θ_{12} independent of longitudinal boost
  - Minimize the impact of incoming quark transverse momentum
- Rotate around the x-axis by π for events with $y_Z < 0$:
  - Avoid possible dilutions by the initial state swapped processes
  - Angular coefficients have symmetric y_Z distributions

$$\int d\Phi_4(k_l, k_{\bar{l}}, k_\chi, k_{\bar{\chi}}) = \int \frac{ds_Z}{2\pi}\frac{ds_X}{2\pi}\int d\Phi_2'(p_Y, p_Z)d\Phi_2(k_l, k_{\bar{l}})d\Phi_2(k_\chi, k_{\bar{\chi}}),$$

$$\int d\Phi_2'(p_Y, p_Z) = \int \frac{d^3p_Z}{(2\pi)^3 2p_Z^0}\frac{d^3p_Y}{(2\pi)^3 2p_Y^0}(2\pi)^4\delta^4(p_1 + p_2 - p_Z - p_Y),$$

$$= \frac{1}{4\pi s}\int \boxed{dy_Z dy_Y dq_T} \cdot q_T$$

$$\boxed{\delta(x_1 - \frac{x_{T,Z}}{2}e^{y_Z} - \frac{x_{T,Y}}{2}e^{y_Y})\delta(x_2 - \frac{x_{T,Z}}{2}e^{-y_Z} - \frac{x_{T,Y}}{2}e^{-y_Y})}$$

$$\int d\Phi_2(k_1, k_2) = \frac{1}{8\pi}\bar{\beta}(\frac{m_1^2}{s_{12}}, \frac{m_2^2}{s_{12}})\frac{d\cos\theta}{2}\frac{d\phi}{2\pi},$$

$$\bar{\beta}(a, b) = \sqrt{\lambda(1, a, b)} = \sqrt{1 + a^2 + b^2 - 2a - 2b - 2ab}.$$

$$x_{T,Z} = \frac{2\sqrt{s_Z + q_T^2}}{\sqrt{s}},\ x_{T,Y} = \frac{2\sqrt{s_Y + q_T^2}}{\sqrt{s}}$$

Parametrization of the lepton angular distribution

We consider the Z boson decay as a probe of the underlying production structure with a narrow width approximation.

$$\frac{d\sigma}{dy_Z dq_T ds_Y d\Phi_2(k_\chi, k_{\bar\chi}) d\cos\theta d\phi} = \frac{d\sigma_P}{dy_Z dq_T ds_Y d\Phi_2(k_\chi, k_{\bar\chi})} \cdot \mathrm{Br}(Z \to l^+ l^-) \cdot 3 \sum_{s,s'} \boxed{\rho^{\mathrm{P}}_{ss'} \rho^{\mathrm{D}}_{ss'}}$$

$$\mathrm{Tr}\rho^{\mathrm{P}} = \int_{\mathcal{R}} d\Phi_2'(p_Y, p_Z) d\Phi_2(k_\chi, k_{\bar\chi}) \sum_{a,b} f_a(x_1, \mu_F) f_b(x_2, \mu_F) \frac{1}{2\hat{s}} \overline{\sum_{\mathrm{ext}}} \sum_s |\mathcal{M}_s|^2 ,$$

$$\boxed{\rho^{\mathrm{P}}_{ss'}} = \frac{1}{\mathrm{Tr}\rho^{\mathrm{P}}} \int_{\mathcal{R}} d\Phi_2'(p_Y, p_Z) d\Phi_2(k_\chi, k_{\bar\chi}) \sum_{a,b} f_a(x_1, \mu_F) f_b(x_2, \mu_F) \frac{1}{2\hat{s}} \overline{\sum_{\mathrm{ext}}} \mathcal{M}_s \mathcal{M}^*_{s'}$$

Angular coefficients

$$\boxed{\rho^{\mathrm{P},CS}_{ss'}} = \sum_{\alpha,\beta} d^{J=1}_{\alpha s}(-\omega) d^{J=1}_{\beta s'}(-\omega) \rho^{\mathrm{P},HEL}_{\alpha\beta}$$

$$\cos\omega = \frac{2\sqrt{\tau_Z}\sinh y_Z}{\sqrt{x^2_{\mathrm{T,Z}}\cosh^2 y_Z - 4\tau_Z}},$$

Parameter	Value
$\sin^2\theta_W$	0.23129
$1/\alpha$	127.95
m_Z	91.1876 GeV
Γ_Z	2.4952 GeV
m_W	$m_Z \cos\theta_W$
Br(Z→ll), l=e,μ	6.73%
μ_F	$E_T = \sqrt{s_Z + q_T^2}$

- Analytic implementation (ALOHA generated HELAS subroutines): allows application of matrix element method (MEM).
- All evaluated angular coefficients checked with toy measurements based on MadGraph5 generated events.

We will show $y_Z - q_T$ distributions of A_{0-4} in different scenarios

$$\frac{\mathrm{d}\sigma}{\mathrm{d}q_\mathrm{T}\mathrm{d}y_\mathrm{Z}\mathrm{d}s_\mathrm{Z}\mathrm{d}\cos\theta\mathrm{d}\phi} = \left(\int \mathrm{d}\cos\theta\mathrm{d}\phi\frac{\mathrm{d}\sigma}{\mathrm{d}q_\mathrm{T}\mathrm{d}y_\mathrm{Z}\mathrm{d}s_\mathrm{Z}\mathrm{d}\cos\theta\mathrm{d}\phi}\right)\frac{3}{16\pi}$$
$$\left\{(1+\cos^2\theta)+\frac{1}{2}A_0(1-3\cos^2\theta)+A_1\sin 2\theta\cos\phi\right.$$
$$\left.+\frac{1}{2}A_2\sin^2\theta\cos 2\phi + A_3\sin\theta\cos\phi + A_4\cos\theta\right\}$$

Angular coefficients in simplified models

- **SM ZZ→2l 2v background**
- **Spin-0 mediator**
- **Spin-1 mediator**
- **Spin-2 mediator**

Angular coefficients in simplified models

Spin-0 mediator

$$\mathcal{L}^{Y_0}_{SMEW} = \frac{1}{\Lambda} g^S_{h3} (D^\mu \phi)^\dagger (D_\mu \phi) Y_0 + \frac{1}{\Lambda} B_{\mu\nu} \left(g^S_B B^{\mu\nu} + g^P_B \tilde{B}^{\mu\nu} \right) Y_0 + \frac{1}{\Lambda} W^i_{\mu\nu} \left(g^S_W W^{i,\mu\nu} + g^P_W \tilde{W}^{i,\mu\nu} \right) Y_0,$$

$$\mathcal{L}^{Y_0}_X = \mathrm{m}_{X_C} g^S_{X_C} X^*_C X_C Y_0 + \bar{\chi}_D (g^S_{X_D} + i g^P_{X_D} \gamma_5) \chi_D Y_0,$$

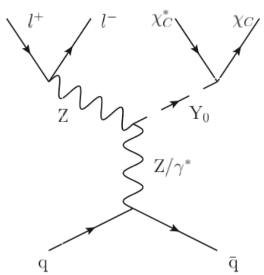

Benchmark	$S0_a$	$S0_b$	$S0_c$
$g^S_{X_D}$	1	0	0
$g^P_{X_D}$	0	1	0
$g^S_{X_C}$	0	0	1
g^S_W	0.25	0	0
g^P_W	0	0.25	0
g^S_{h3}	0	0	1
Λ (GeV)	3000	3000	3000
Interaction	CP-even	CP-odd	CP-even
m_χ (GeV)	10	10	10
m_{Y_0} (GeV)	1000	1000	1000
Γ_{Y_0} (GeV)	41.4	41.4	1.05
Cross section (fb)	0.0103	0.00977	2.98e-08

Spin-1 mediator

$$\mathcal{L}^{Y_1}_{X_D} = \bar{\chi}_D \gamma_\mu \left(g^V_{X_D} + g^A_{X_D} \gamma_5 \right) \chi_D Y_1^\mu$$

$$\mathcal{L}^{Y_1}_{SM} = \bar{d}_i \gamma_\mu \left(g^V_{d_{ij}} + g^A_{d_{ij}} \gamma_5 \right) d_j Y_1^\mu + \bar{u}_i \gamma_\mu \left(g^V_{u_{ij}} + g^A_{u_{ij}} \gamma_5 \right) u_j Y_1^\mu$$

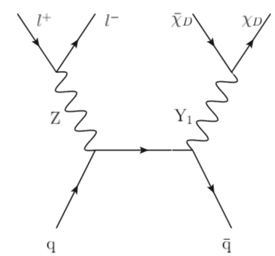

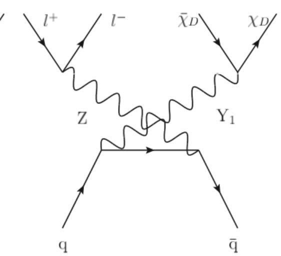

Benchmark	$S1_a$ Spin independent	$S1_b$ Right handed	$S1_c$ Left handed	$S1_0$ SM ($ZZ \to 2l2\nu$)
$g^V_{X_D}$	1	$1/\sqrt{2}$	$1/\sqrt{2}$	-
$g^A_{X_D}$	0	$1/\sqrt{2}$	$-1/\sqrt{2}$	-
$g^V_{X_C}$	0	0	0	-
g^V_u	0.25	$\sqrt{2}/8$	$\sqrt{2}/8$	-
g^A_u	0	$\sqrt{2}/8$	$-\sqrt{2}/8$	-
g^V_d	0.25	$\sqrt{2}/8$	$\sqrt{2}/8$	-
g^A_d	0	$\sqrt{2}/8$	$-\sqrt{2}/8$	-
m_χ (GeV)	10	10	10	-
m_{Y_1} (GeV)	1000	1000	1000	-
Γ_{Y_1} (GeV)	56.3	55.9	55.9	-
Cross section (fb)	2.50	0.533	4.50	239

Spin-2 mediator

$$\mathcal{L}^{Y_2}_X = -\frac{1}{\Lambda} g^T_X \, T^X_{\mu\nu} Y_2^{\mu\nu}$$

$$\mathcal{L}^{Y_2}_{\mathrm{SM}} = -\frac{1}{\Lambda} \sum_i g^T_i \, T^i_{\mu\nu} Y_2^{\mu\nu}$$

Benchmark	$S2_a$	$S2_b$	$S2_c$
$g^T_{X_D}$	1	0	0
$g^T_{X_R}$	0	1	0
$g^T_{X_V}$	0	0	1
g^T_{SM}	1	1	1
m_χ (GeV)	10	10	10
m_{Y_2} (GeV)	1000	1000	1000
Λ	3000	3000	3000
Γ_{Y_2} (GeV)	95.3	93.7	97.7
Cross section (fb)	2.73	0.0462	0.578

- *JHEP 02 (2016) 082*
- *Report of the ATLAS/CMS Dark Matter Forum, 1507.00966*
- *Eur. Phys. J. C77 (2017) 326*

Angular coefficients in simplified models

$y_Z - q_T$ differential cross section

Clear differences among models, but only 2-dimension

It's worth looking into the angular distribution and look for further information.

SM ZZ→2l2ν

Spin-0 mediator (a-c)

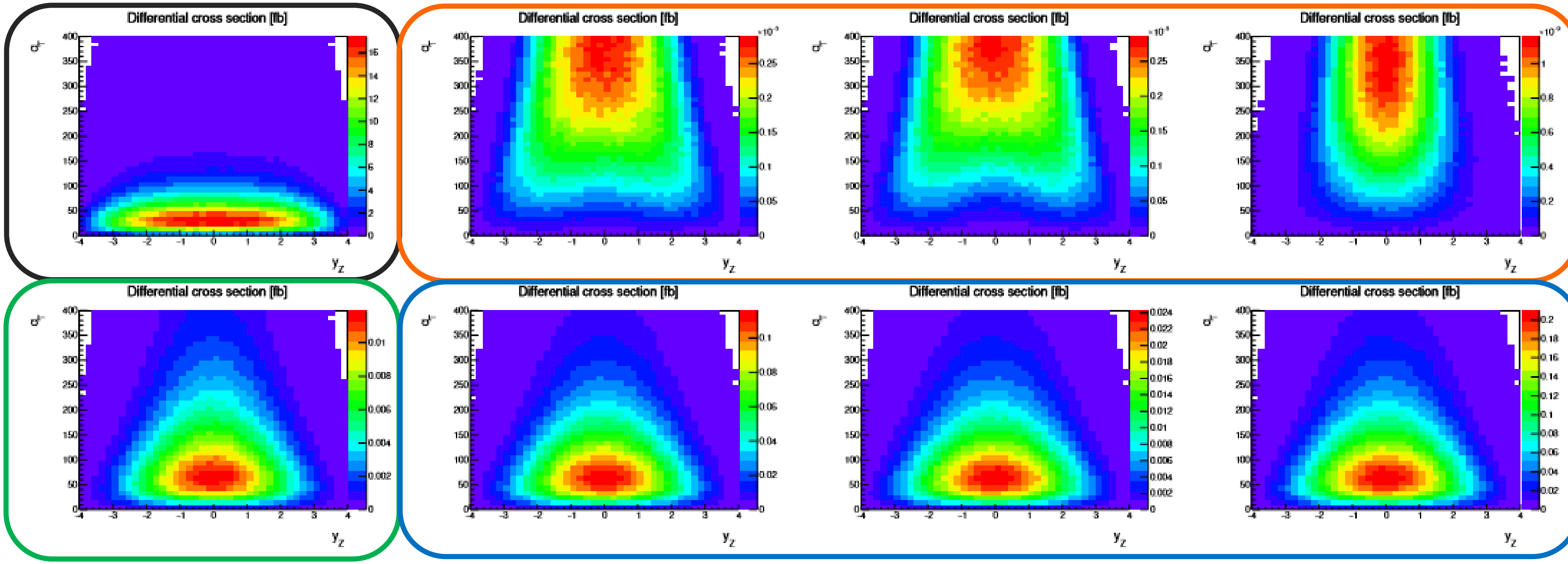

Spin-2 mediator

Spin-1 mediator (a-c)

A0 in the $y_Z - q_T$ plane

SM ZZ→2l2ν

Spin-0 mediator (a-c)

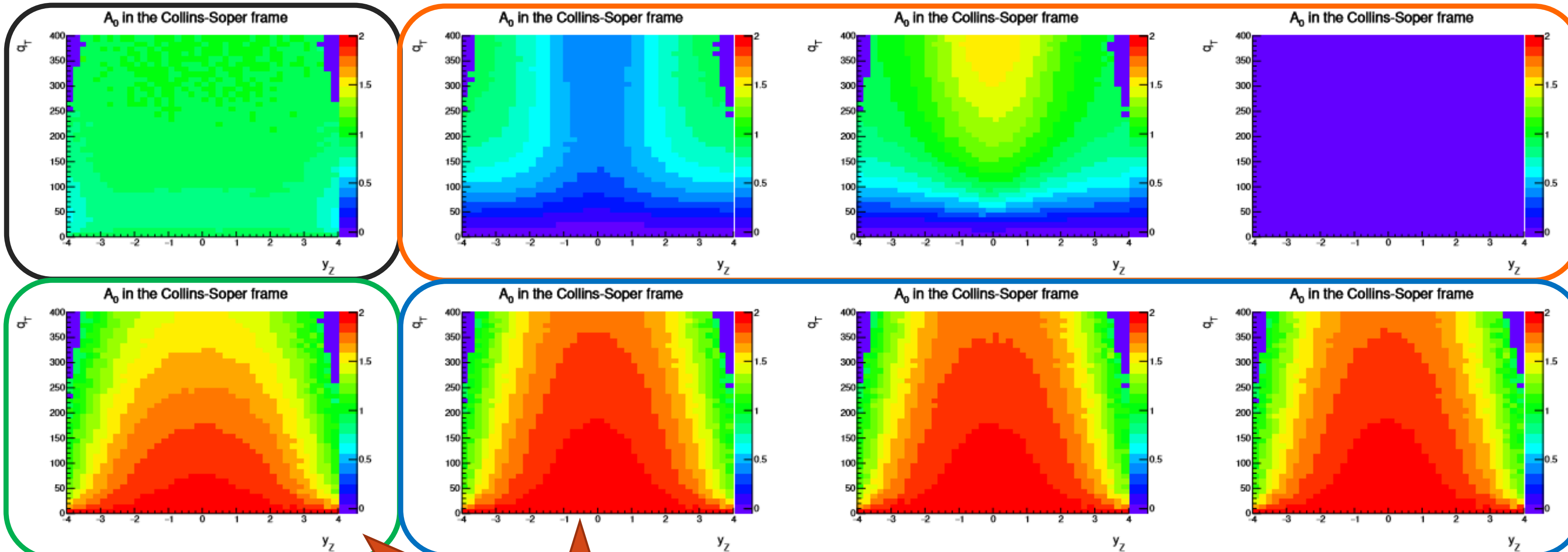

Spin-2 mediator

Spin-1 mediator (a-c)

The A0 distribution can distinguish spins of the mediators

Angular coefficients in simplified models

A1 in the $y_Z - q_T$ plane

SM ZZ→2l2ν

Spin-0 mediator (a-c)

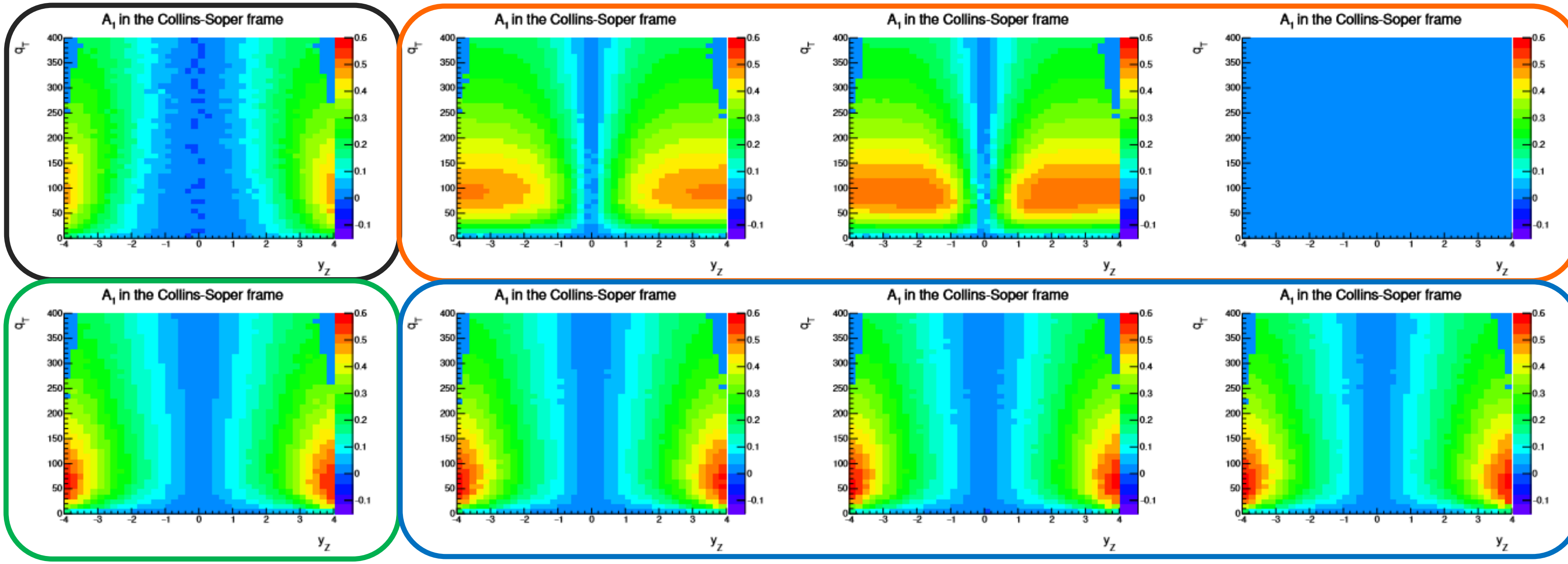

Spin-2 mediator

Spin-1 mediator (a-c)

Distributions look similar
Exception: A1 in S0c = 0

A2 in the $y_Z - q_T$ plane

SM ZZ→2l2ν

Spin-0 mediator (a-c)

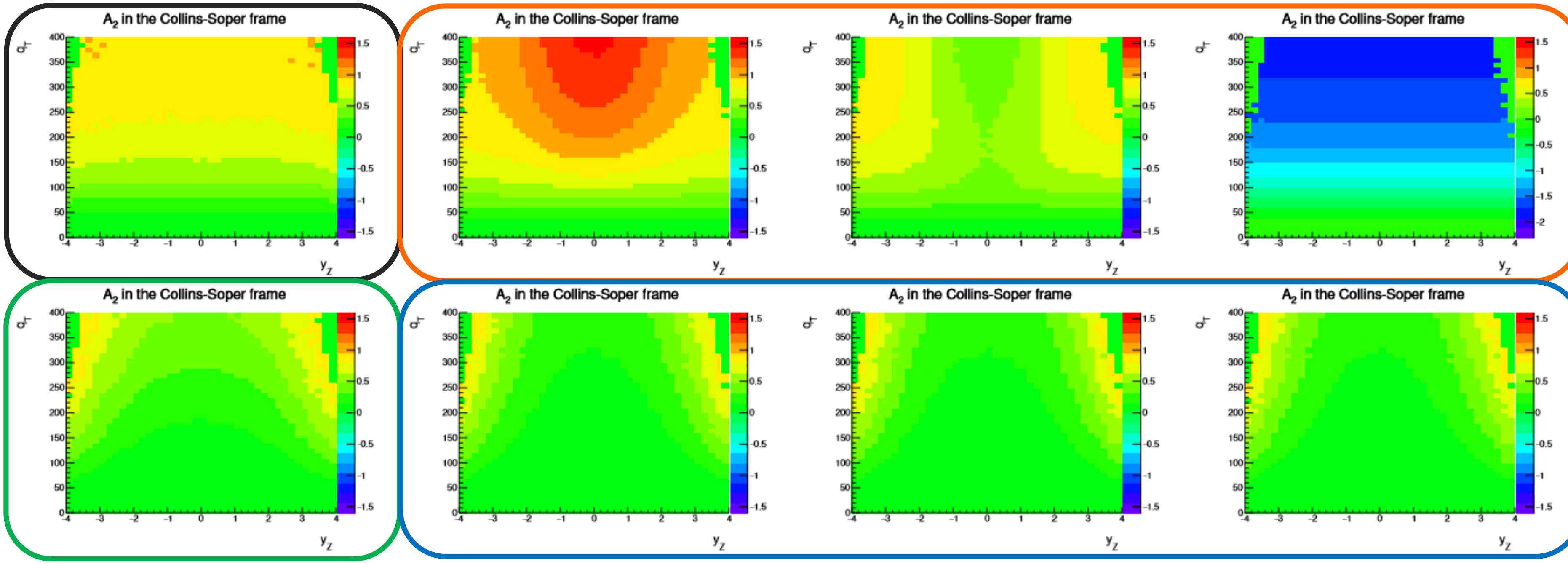

Spin-2 mediator

Spin-1 mediator (a-c)

Sensitive to spin-0 models
Spin-2 signature similar but different from the one of the spin-1 model

Angular coefficients in simplified models

A3 in the $y_Z - q_T$ plane

SM ZZ→2l2ν

Spin-0 mediator (a-c)

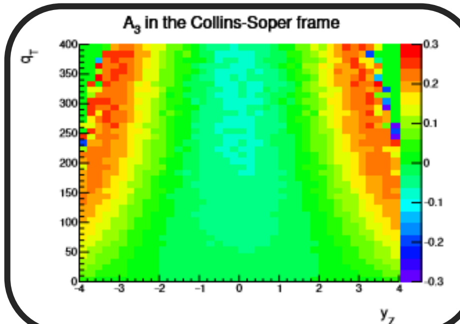

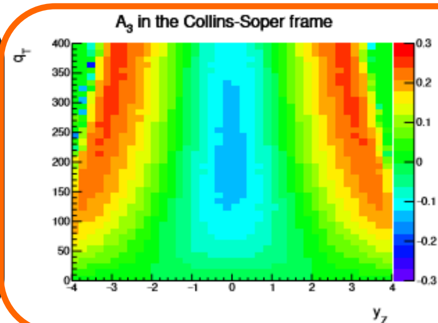

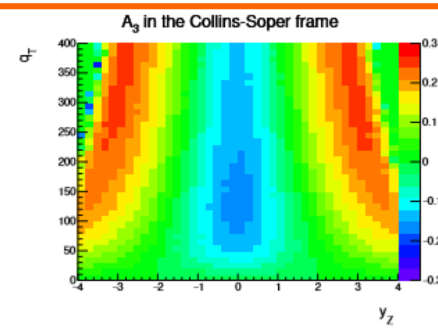

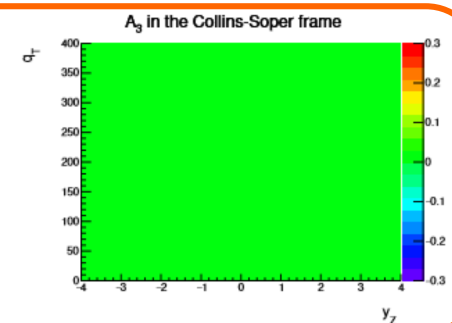

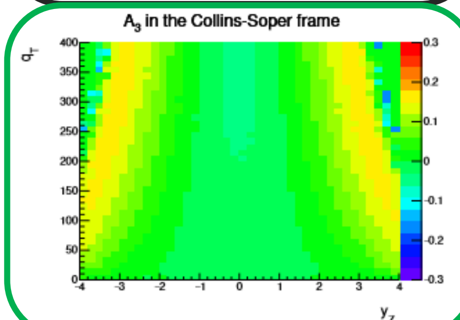

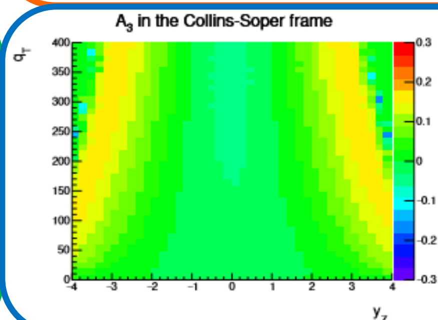

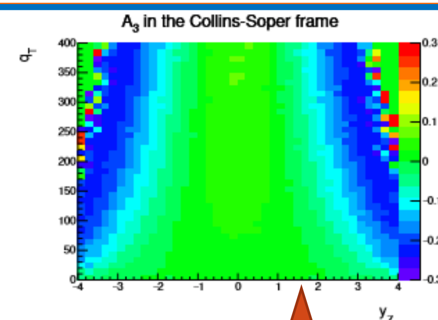

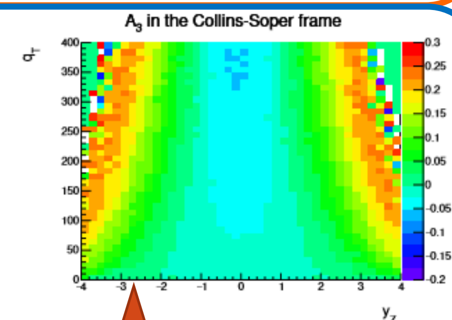

Spin-2 mediator

Spin-1 mediator (a-c)

A3, **A4**: Sensitive to the left- and right- handed couplings

Angular coefficients in simplified models

A4 in the $y_Z - q_T$ plane

SM ZZ→2l2ν

Spin-0 mediator (a-c)

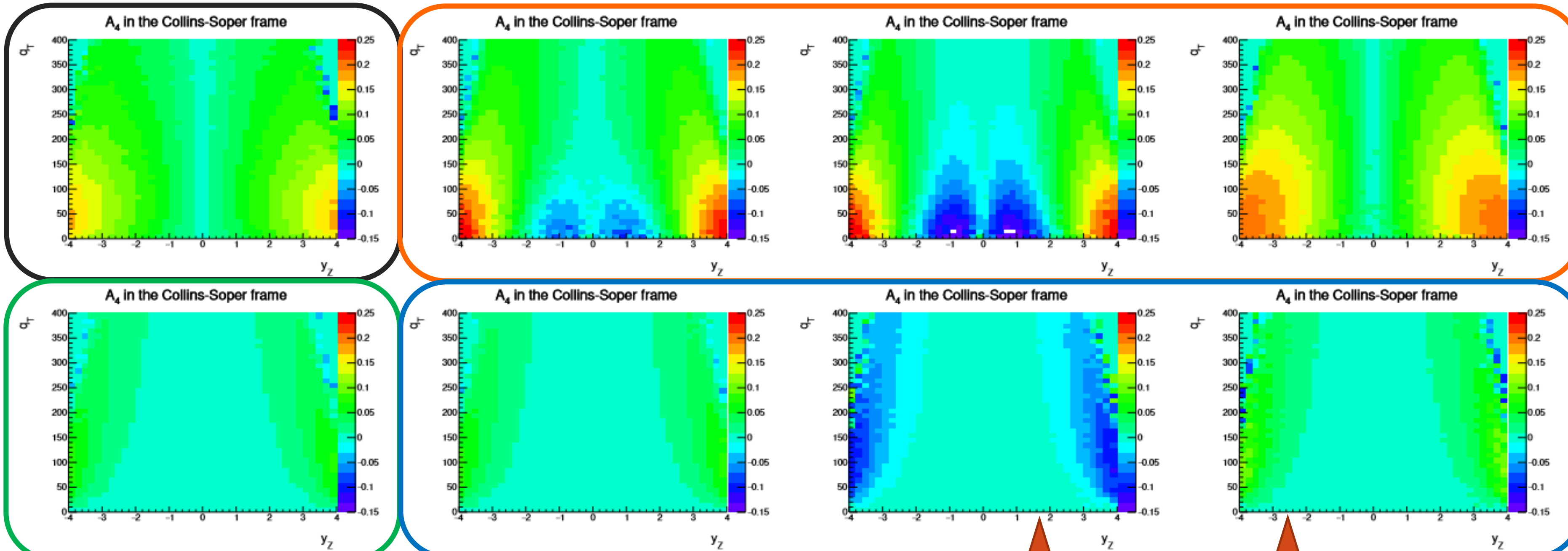

Spin-2 mediator

Spin-1 mediator (a-c)

A3, **A4**: Sensitive to the left- and right- handed couplings

Visible part: $\mathbf{x} = (y_Z, q_T, \cos\theta_{CS}, \phi_{CS})$

Invisible part (integrated): $(y_Y, s_Y, \cos\theta_\chi, \phi_\chi)$

Limits on the coupling strength parameters and multivariate discriminator

- **Benchmark scenarios S0a, S0b, S0c**
- **Benchmark scenarios S1a, S1b, S1c**

Setting limits on the coupling strength parameters

We exploit a dynamically constructed matrix element based likelihood function to set limits on the coupling strength parameters:

$$\rho(\mathbf{p}^{\mathrm{vis}}|\lambda) = \frac{1}{\sigma_\lambda} \sum_{a,b} \int \mathrm{d}x_1 \mathrm{d}x_2 f_a(x_1, \mu_{\mathrm{F}}) f_b(x_2, \mu_{\mathrm{F}}) \int \mathrm{d}\Phi \frac{\mathrm{d}\hat{\sigma}}{\mathrm{d}\Phi} \prod_{i \in \mathrm{vis}} \delta(\mathbf{p}_i - \mathbf{p}_i^{vis})$$

Visible part: $\mathbf{x} = (y_{\mathrm{Z}}, q_{\mathrm{T}}, \cos\theta_{CS}, \phi_{CS})$

Invisible part (integrated): $(y_{\mathrm{Y}}, s_{\mathrm{Y}}, \cos\theta_\chi, \phi_\chi)$

λ scales couplings of the dark mediator to the dark matter and the SM particles at the same time

An unbinned likelihood fit is performed to extract limit

$$\mathcal{L}(\mathrm{data}|\lambda, \boldsymbol{\theta}) = \mathrm{Poisson}(N|S(\lambda, \boldsymbol{\theta}) + B(\boldsymbol{\theta}))\rho(\boldsymbol{\theta}) \prod_i \rho(\mathbf{x}^i|\lambda, \boldsymbol{\theta}),$$

$$\rho(\mathbf{x}|\lambda, \boldsymbol{\theta}) = \frac{S(\lambda, \boldsymbol{\theta})\rho_s(\mathbf{x}^i, \lambda) + B(\boldsymbol{\theta})\rho_b(\mathbf{x}^i)}{S(\lambda, \boldsymbol{\theta}) + B(\boldsymbol{\theta})},$$

Evaluate test statistics in the large sample limit

Dual integration, 4-dim for each step (700x6 CPU hours, 2.4 GHz)

- Integrate over the invisible part
- Evaluate the KL divergence term

$$t_\lambda = -2\ln \frac{\mathcal{L}(\mathrm{data}|\lambda, \hat{\boldsymbol{\theta}}_\lambda)}{\mathcal{L}(\mathrm{data}|\hat{\lambda}, \hat{\boldsymbol{\theta}})}$$

$$\begin{aligned} t_\lambda &\xrightarrow{N\to\infty} -2\ln \frac{\mathrm{Poisson}(N|S(\lambda)+B)}{\mathrm{Poisson}(N|B)} + 2N \int \mathrm{d}\mathbf{x} \rho(\mathbf{x}|\lambda=0) \ln \frac{\rho(\mathbf{x}|\lambda=0)}{\rho(\mathbf{x}|\lambda)} \\ &= -2\ln \frac{\mathrm{Poisson}(N|S(\lambda)+B)}{\mathrm{Poisson}(N|B)} + 2N \cdot D(\rho(\mathbf{x}|\lambda=0)||\rho(\mathbf{x}|\lambda)). \end{aligned}$$

Setting limits on the coupling strength parameters

Background modeling and event selections

Consider the same selections as in the 13 TeV CMS measurement:
JHEP 03 (2017) 061

Selections implemented in numerical integration (BL-selections):

Variable	Requirements
p_T^l	> 20 GeV
s_Z	NWA
E_T^{miss}	> 80 GeV
$\lvert\eta_l\rvert$	< 2.4
ΔR_{ll}	> 0.4
$\lvert y_Z\rvert$	< 2.5

Distributions distorted by selections. Shown for background only hypothesis

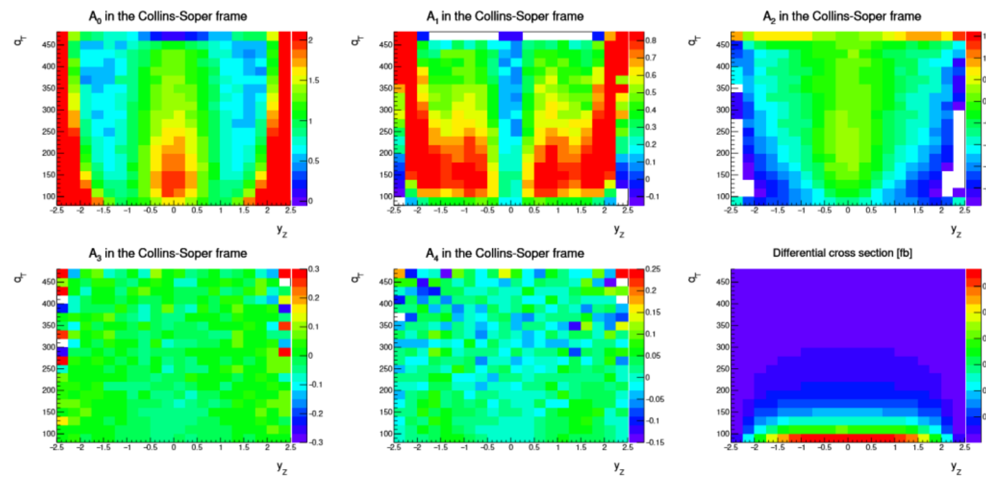

Other selection effects are included through an ancillary $A \cdot \epsilon$ factor.
Event rate corresponds to 13 TeV LHC with 150 fb^{-1} data.

	Process	Cross section with BL-selections (fb)	Ancillary $A \cdot \epsilon$	Events
Matrix Element	$ZZ \to 2l2\nu$	27.7	0.488	2028
Phase space	Non-resonant-ll	1.57×10^3	5.80×10^{-3}	1370
Matrix Element	$WZ(\to e\nu 2l)$	17.05	0.296	757
Matrix Element	$Z/\gamma^* \to l^+l^-$	3.61×10^4	1.23×10^{-4}	665

Setting limits on the coupling strength parameters

Upper limits on the coupling strength parameters of the S0 benchmark scenarios.

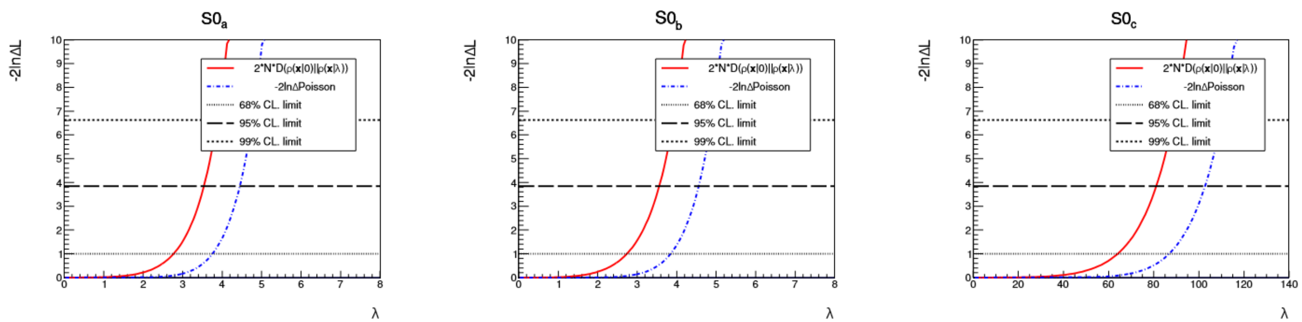

Upper limits on the coupling strength parameters of the S1 benchmark scenarios.

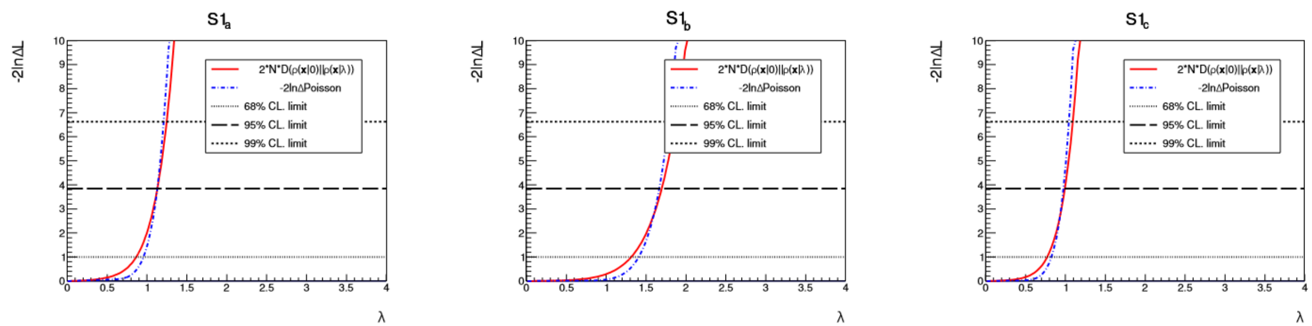

Benchmark	$S0_a$	$S0_b$	$S0_c$	$S1_a$	$S1_b$	$S1_c$
Limit from the normalization term (λ_1)	4.4	4.6	103	1.1	1.7	0.97
Signal cross section at λ_1 (fb)	1.86	1.87	1.86	1.87	1.87	1.87
Limit from the KL-divergence term (λ_2)	3.5	3.6	81	1.1	1.7	0.99
Signal cross section at λ_2 (fb)	0.75	0.70	0.72	1.9	2.0	2.0
Combined limit (λ_0)	3.5	3.5	79	1.0	1.5	0.89

Close

Quantify the shape improvements

Matrix Element Kinematic Discriminator (MEKD)

We have constructed an example MEKD
- A kind of multivariate analysis motivated by theory
- Applicable regardless of the source of data

$$\mathrm{MEKD} = \ln \frac{\rho_s(\mathbf{x}, \lambda)}{\rho_b(\mathbf{x})}$$

Example application using MadGraph generated events

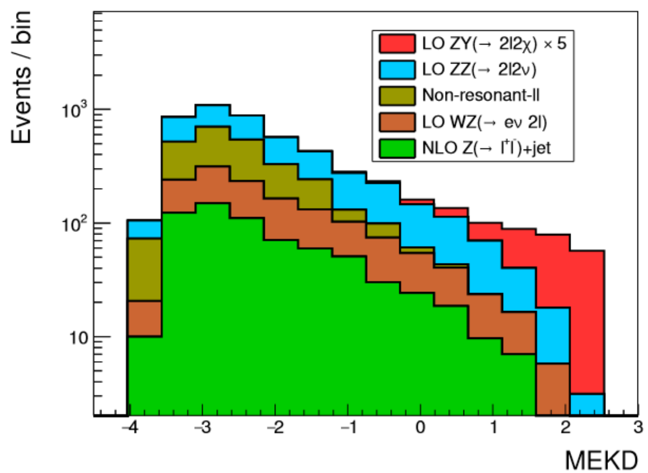

MG5 LO samples

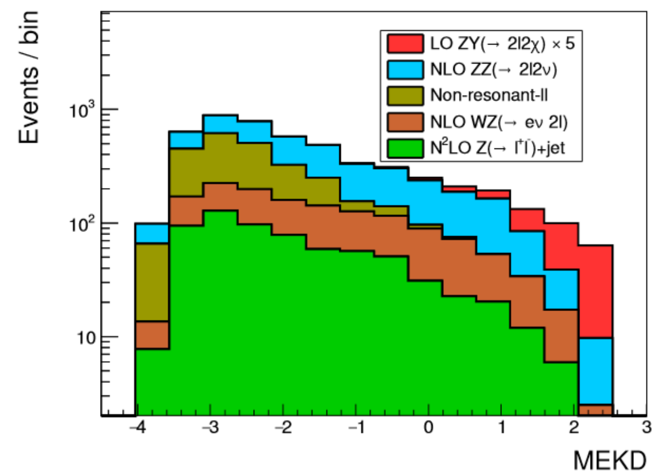

NLO samples for major backgrounds

Thanks for your attention!

21 BACKUP

Angular distribution and the production density matrix

$$\rho = \frac{1}{3}(1+\sqrt{3}\sum_{k=1}^{8} P_k\lambda_k) = \frac{1}{3} + \frac{1}{\sqrt{3}} \begin{array}{cc} \begin{array}{ccc} + & - & 0 \end{array} & \\ \begin{pmatrix} P_3+\frac{P_8}{\sqrt{3}} & P_1-iP_2 & P_4-iP_5 \\ P_1+iP_2 & -P_3+\frac{P_8}{\sqrt{3}} & P_6-iP_7 \\ P_4+iP_5 & P_6+iP_7 & \frac{-2P_8}{\sqrt{3}} \end{pmatrix} & \begin{array}{c} + \\ - \\ 0 \end{array} \end{array}$$

where $\lambda_k s$ are Gell-Mann matrices

We study the production density matrix in the parton-parton center of mass frame

- Helicity amplitudes calculated
- Analytic expression for production density matrix as a function of $\sqrt{\hat{s}}$ and $\cos\theta$
- P= $\sqrt{\sum_k P_k^2}$ invariant in qt - (yz-yj) plane

P= $\sqrt{\mathbf{tr}(\rho^2)}$=$\sqrt{\sum_k P_k^2}$=1 for pure state;
<1 for mixed state

Unpolarized vs. Total rate

$$4\pi tr\left(\rho_{Prod}\rho^T_{Decay}\right) = 4\pi\sum_{\lambda,\lambda'}\rho^{\lambda\lambda'}_{Prod}(\cos\hat{\theta},\hat{s})\rho^{\lambda\lambda'}_{Decay}(\theta,\phi) = 1 + \frac{P_8}{2}(1-3\cos^2\theta) +$$
$$\frac{\sqrt{3}}{2\sqrt{2}}(P_4-P_6)\sin 2\theta\cos\phi + \frac{\sqrt{3}}{2}P_1\sin^2\theta\cos 2\phi$$
$$-\sqrt{3}\frac{c^2_{L,l}-c^2_{R,l}}{c^2_{L,l}+c^2_{R,l}}P_3\cos\theta - \sqrt{\frac{3}{2}}\frac{c^2_{L,l}-c^2_{R,l}}{c^2_{L,l}+c^2_{R,l}}(P_4+P_6)\sin\theta\cos\phi$$
$$-\sqrt{\frac{3}{2}}\frac{c^2_{L,l}-c^2_{R,l}}{c^2_{L,l}+c^2_{R,l}}(P_5-P_7)\sin\theta\sin\phi + \frac{\sqrt{3}}{2\sqrt{2}}(P_5+P_7)\sin 2\theta\sin\phi + \frac{\sqrt{3}}{2}P_2\sin^2\theta\sin 2\phi.$$

$$\boxed{P8 = \frac{1}{2} - \frac{3}{4}A0}$$

Kinematics

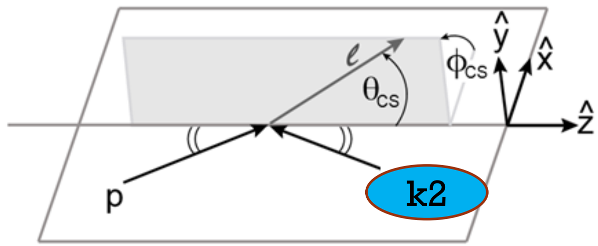

There are two ways to go to the Z boson rest frame
But, parton-parton c.m. frame can not be obtained in experiment

Left flying parton momentum k2	Frame-I (boost from Lab. frame)	Frame-II (boost from parton-parton c.m. frame)
Helicity frame	$x_2 \frac{\sqrt{s}}{2} \frac{1}{\sqrt{\bar{x}_T^2 \cosh^2 y_Z - 4\tau}} \begin{pmatrix} \sqrt{\bar{x}_T^2 \cosh^2 y_Z - 4\tau}\, \frac{\bar{x}_T e^{y_Z}}{2\sqrt{\tau}} \\ x_T \\ 0 \\ -\frac{\bar{x}_T^2 e^{2y_Z} + x_T^2 - 4\tau}{4\sqrt{\tau}} \end{pmatrix}$	$\frac{\sqrt{\hat{s}}}{4\sqrt{\hat{\tau}}} \begin{pmatrix} (1+\cos\hat{\theta}) + (1-\cos\hat{\theta})\hat{\tau} \\ \sin\hat{\theta} \\ 0 \\ -(1+\cos\hat{\theta}) + (1-\cos\hat{\theta})\hat{\tau} \end{pmatrix}$
Beam-direction frame	$\frac{x_2 s}{4 m_Z} \bar{x}_T e^{y_Z} \begin{pmatrix} 1 \\ -\frac{4\sqrt{\tau}}{\bar{x}_T^2} \\ 0 \\ \frac{\bar{x}_T^2 - 4\tau}{\bar{x}_T^2} \end{pmatrix}$	$\frac{\hat{s}}{4 m_Z}((1+\cos\hat{\theta}) + (1-\cos\hat{\theta})\hat{\tau}) \begin{pmatrix} 1 \\ -\frac{4\sqrt{\tau}}{\bar{x}_T^2} \\ 0 \\ \frac{\bar{x}_T^2 - 4\tau}{\bar{x}_T^2} \end{pmatrix}$
Collins-Soper frame	$\frac{x_2 s}{4 m_Z} e^{y_Z} \bar{x}_T \boxed{(1, -\sqrt{1-c}, 0, -\sqrt{c})}$	$\frac{m_Z}{2a} \boxed{(1, -\sqrt{1-c}, 0, \sqrt{c})}$

a,b,c are parton-parton center of mass frame scaling variables

Collins-Soper frame has advantage also for high pT Z boson study